Electronic Dependence of C−O Reductive Elimination from Palladium (Aryl)neopentoxide Complexes

Ross A. Widenhoefer[1] and Stephen L. Buchwald*

Contribution from the Department of Chemistry, Massachusetts Institute of Technology, Cambridge, Massachusetts 02139

Received February 27, 1998

Abstract: Thermal decomposition of the palladium (aryl)neopentoxide complexes [P−P]Pd(Ar)OCH_2CMe_3 [P−P = Tol-BINAP or BINAP; Ar = *p*-C_6H_4CHO (**1b**), *p*-C_6H_4COPh (**1c**), *p*-$C_6H_4NO_2$ (**1d**), *o*-$C_6H_4NO_2$ (**1e**), *o*-C_6H_4CN (**1f**)] possessing substituents on the palladium-bound aryl group suitable for delocalization of negative charge led to quantitative (≥95%) formation of aryl ether without detectable *β*-hydride elimination. Thermal decomposition of **1b**−**f** obeyed first-order kinetics, and the rate of reductive elimination decreased in the order *o*-NO_2 > *p*-NO_2 > *p*-CHO > *p*-COPh > *o*-CN. Conversely, thermal decomposition of the related derivatives [P−P]Pd(Ar)OCH_2CMe_3 [P−P = Tol-BINAP or BINAP; Ar = *p*-C_6H_4Cl (**1g**), *m*-$C_6H_4NO_2$ (**1h**), *m*-C_6H_4CN (**1i**)] which did not possess a resonance stabilizing group on the palladium-bound aryl group led to no detectable formation of aryl ether. These and related data point to the buildup of negative charge in the palladium-bound aryl group in the transition state for C−O reductive elimination and are consistent with a mechanism initiated by inner-sphere nucleophilic attack of the alkoxide ligand at the ipso-carbon atom of the palladium-bound aryl group through a zwitterionic Meisenheimer-type intermediate or transition state.

Introduction

In conjunction with our development of catalytic C−O bond-forming protocols,[2] we recently reported some rare examples of C−O reductive elimination from palladium alkoxide complexes.[3−5] For example, thermolysis of the palladium (*p*-cyanophenyl)neopentoxide complex [Tol-BINAP]Pd(*p*-C_6H_4-CN)(OCH_2CMe_3) (**1a**) [Tol-BINAP = 2,2′-bis(di-*p*-tolylphosphino)-1,1′-binaphthyl] in THF-d_8 at 47 °C led to C−O reductive elimination with formation of *p*-neopentoxybenzonitrile (85%). Thermolysis of **1a** also led to formation of 4,4′-dimethylbiphenyl (16%) via a secondary P−C bond cleavage process. Kinetic analysis of the decomposition of **1a** in the presence of excess potassium neopentoxide was consistent with reductive elimination via competing alkoxide-dependent and alkoxide-independent pathways. An alkoxide-dependent pathway, initiated by direct attack of $KOCH_2CMe_3$ at palladium, was supported by the presence of an associative alkoxide exchange pathway for **1a**, although direct attack of the alkoxide at the ipso-carbon atom of the palladium-bound *p*-cyanophenyl group was also consistent with our kinetic data.

Scheme 1

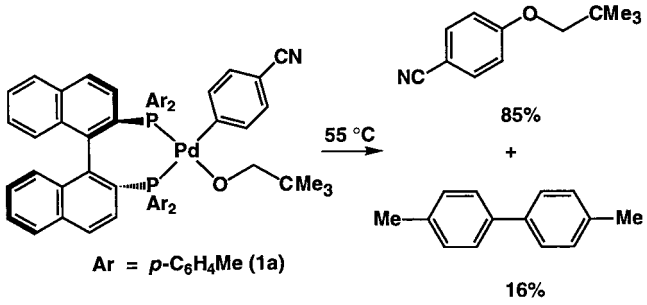

Several observations regarding the alkoxide-independent reductive elimination pathway appeared inconsistent with the concerted, symmetric three-centered mechanism[6] typically invoked for C−C[7] and C−H[8] reductive elimination from group 10 metal complexes (Scheme 2, path a). In particular, C−O reductive elimination from aryl(alkoxide) complexes occurred readily while aryl(aryloxide) derivatives were virtually resistant to reductive elimination.[3] This behavior seemed unusual for concerted reductive elimination[9] but appeared to parallel the nucleophilicity of the corresponding OR ligand. Therefore, we

(1) Present address: Paul M. Gross Chemical Laboratories, Duke University, Durham, NC 27708-0346.

(2) (a) Palucki, M.; Wolfe, J. P.; Buchwald, S. L. *J. Am. Chem. Soc.* **1996**, *118*, 10333. (b) Palucki, M.; Wolfe, J. P.; Buchwald, S. L. *J. Am. Chem. Soc.* **1997**, *119*, 3395.

(3) Widenhoefer, R. A.; Zhong, H. A.; Buchwald, S. L. *J. Am. Chem. Soc.* **1997**, *119*, 6787.

(4) For other examples of C−O reductive elimination, see: (a) Komiya, S.; Akai, Y.; Tanaka, K.; Yamamoto, T.; Yamamoto, A. *Organometallics* **1985**, *4*, 1130. (b) Mann, G.; Hartwig, J. F. *J. Am. Chem. Soc.* **1996**, *118*, 13109. (c) Koo, K.; Hillhouse, G. L.; Rheingold, A. L. *Organometallics* **1995**, *14*, 456. (d) Matsunaga, P. T.; Mavropoulos, J. C.; Hillhouse, G. L. *Polyhedron* **1995**, *14*, 175. (e) Han, R.; Hillhouse, G. L. *J. Am. Chem. Soc.* **1997**, *119*, 8135.

(5) (a) For examples of C−S reductive elimination, see: Barañano, D.; Hartwig, J. F. *J. Am. Chem. Soc.* **1995**, *117*, 2937. (b) For examples of C−N reductive elimination, see: Driver, M. S.; Hartwig, J. F. *J. Am. Chem. Soc.* **1997**, *118*, 8232.

(6) (a) Collman, J. P.; Hegedus, L. S.; Norton, J. R.; Jinke, R. G. In *Principles and Applications of Organotransition Metal Chemistry*; University Science: Mill Valley, CA, 1987; p 322. (b) Stille, J. K. In *The Chemistry of the Metal−Carbon Bond, Vol II. The Nature and Cleavage of the Metal−Carbon Bond*; Hartley, F. R., Patai, S., Eds.; Wiley: New York, 1985; pp 625−787.

(7) (a) Stang, P. J.; Kowalski, M. H. *J. Am. Chem. Soc.* **1989**, *111*, 3356. (b) Braterman, P. S.; Cross, R. J.; Young, G. B. *J. Chem. Soc., Dalton Trans.* **1977**, 1892. (c) Braterman, P. S.; Cross, R. J.; Young, G. B. *J. Chem. Soc., Dalton Trans.* **1977**, 1306.

(8) (a) Michelin, R. A.; Faglia, S.; Uguagliati, P. *Inorg. Chem.* **1983**, *22*, 1831. (b) Abis, L.; Sen, A.; Halpern, J. *J. Am. Chem. Soc.* **1978**, *100*, 2915.

(9) (a) Jones, W. D.; Kuykendall, V. L. *Inorg. Chem.* **1991**, *30*, 2615. (b) Brown, J. M.; Guiry, P. J. *Inorg. Chim. Acta* **1994**, *220*, 249.

S0002-7863(98)00658-1 CCC: $15.00
Published on Web 06/19/1998

Scheme 2

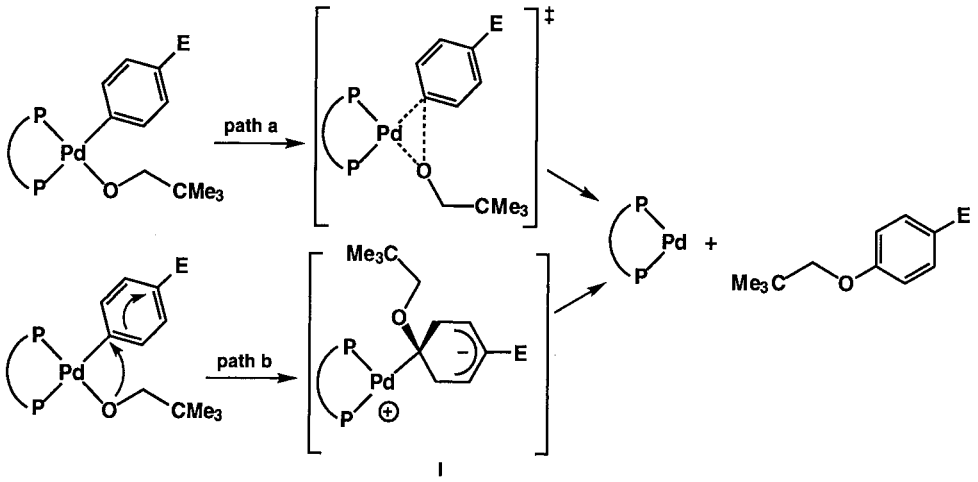

Scheme 3

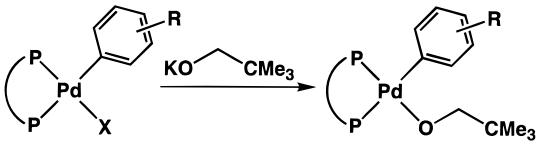

X	P P	R	$L_2Pd(Ar)OR$
Br	BINAP	*p*-CHO	**1b**
Br	BINAP	*p*-COPh	**1c**
I	Tol-BINAP	*p*-NO_2	**1d**
I	BINAP	*o*-NO_2	**1e**
Br	Tol-BINAP	*o*-CN	**1f**
Br	BINAP	*p*-Cl	**1g**
I	Tol-BINAP	*m*-NO_2	**1h**
Br	Tol-BINAP	*m*-CN	**1i**
Br	dppf	*p*-NO_2	**2a**
Br	dppf	*m*-CN	**2b**

considered an alternative mechanism for C−O reductive elimination initiated by inner-sphere attack of the alkoxide ligand at the ipso-carbon atom of the palladium-bound aryl group via a Meisenheimer intermediate or transition state such as **I** (Scheme 2, path b). In an effort to further probe the intimate mechanism of palladium-mediated C−O reductive elimination, we have investigated the rate and efficiency of the thermal decomposition of palladium (aryl)neopentoxide complexes as a function of the electronic nature of the palladium-bound aryl group.

Results

Formation of Palladium (Aryl)neopentoxide Complexes. The palladium (aryl)neopentoxide complexes [P−P]Pd(Ar)-OCH_2CMe_3 [P−P = Tol-BINAP or BINAP; Ar = *p*-C_6H_4CHO (**1b**), *p*-C_6H_4COPh (**1c**), *p*-$C_6H_4NO_2$ (**1d**), *o*-$C_6H_4NO_2$ (**1e**), *o*-C_6H_4CN (**1f**)), *p*-C_6H_4Cl (**1g**), *m*-$C_6H_4NO_2$ (**1h**), *m*-C_6H_4CN (**1i**), (dppf)Pd(*p*-$C_6H_4NO_2$)OCH_2CMe_3, (**2a**) and (dppf)Pd(*m*-C_6H_4CN)OCH_2CMe_3 (**2b**)] [BINAP = 2,2′-bis(diphenylphosphino)-1,1′-binaphthyl; dppf = 1,1′-bis(diphenylphosphino)-ferrocene] were prepared from reaction of the appropriate palladium (aryl)halide complex [P−P]Pd(Ar)X [X = Br, I] and 1 equiv of potassium neopentoxide in THF-d_8 and were characterized without isolation by low-temperature ^{1}H and ^{31}P NMR spectroscopy (Scheme 3). In all cases, the desired alkoxide complex was formed as the exclusive species in quantitative yield (≥95%) as indicated by ^{1}H and ^{31}P NMR spectroscopies.[10] In addition, the *m*-cyanophenyl derivative **1i** was particularly stable and was isolated and characterized by spectroscopy and elemental analysis.

Scheme 4

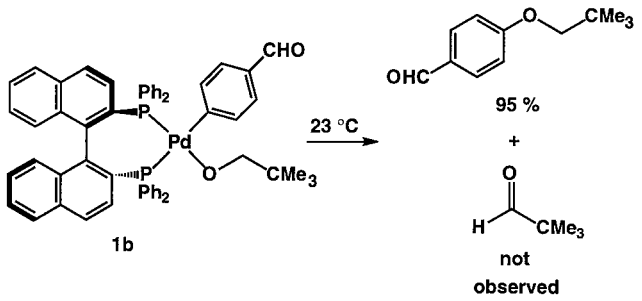

Thermolysis of Palladium (Aryl)alkoxide Complexes. As was previously observed for the *p*-cyanophenyl complex **1a**,[3] thermolysis of the *p*-carboxaldehyde neopentoxide complex **1b** led to C−O reductive elimination without detectable β-hydride elimination. For example, when a THF-d_8 solution of **1b** was warmed from −50 to 23 °C in an NMR probe, **1b** began to decompose. Decomposition of **1b** at 23 °C obeyed first-order kinetics to >3 half-lives with an observed rate constant of $k_{obs} = 1.26 \times 10^{-3}$ s^{-1} ($t_{1/2} = 9.2$ min, $\Delta G^{\ddagger} = 21.4$ kcal mol^{-1}) (Scheme 4, Figure 1, Table 1). ^{1}H NMR and GC analysis of the resulting black solution and comparison with authentic sample revealed the formation of *p*-neopentoxybenzaldehyde in quantitative yield (95 ± 5%). Significantly, the rate of C−O reductive elimination from **1b** was nearly an order of magnitude faster than decomposition of *p*-cyanophenyl derivative **1a** under comparable conditions.[3]

Thermolysis of related derivatives **1c**−**f** led in each case to first-order decay to >3 half-lives with formation of the corresponding aryl ether in quantitative yield.[11] However, the rate of decomposition depended strongly on the nature of the

(10) ^{1}H and ^{31}P NMR spectra of complexes **1b**−**i** were straightforward and were analogous to those of **1a**. However, NMR spectra of *o*-substituted complexes **1e** and **1f** and the corresponding aryl halide complexes [(±)-BINAP]Pd(*o*-$C_6H_4NO_2$)(I) and [(*S*)-Tol-BINAP]Pd(*o*-C_6H_4CN)(Br) were complicated by the presence of two isomers in THF-d_8. For example, [(±)-BINAP]Pd(*o*-$C_6H_4NO_2$)(I) displayed a 3:2 ratio of isomers, [(*S*)-Tol-BINAP]-Pd(*o*-C_6H_4CN)(Br) displayed a 2:1 ratio of isomers, **1e** displayed ~10:1 ratio of isomers at − 55 °C, and **1f** displayed a 2:1 ratio of isomers at 23 °C. These isomers presumably correspond to rotamers generated by hindered rotation of the phosphorus-bound aryl group proximal to the palladium-bound *o*-substituted aryl group. However, [(±)-BINAP]Pd(*o*-$C_6H_4NO_2$)(I) and [(*S*)-Tol-BINAP]Pd(*o*-C_6H_4CN)(Br) displayed a single isomer in $CDCl_3$. The solvent-dependence of isomer formation is not clear.

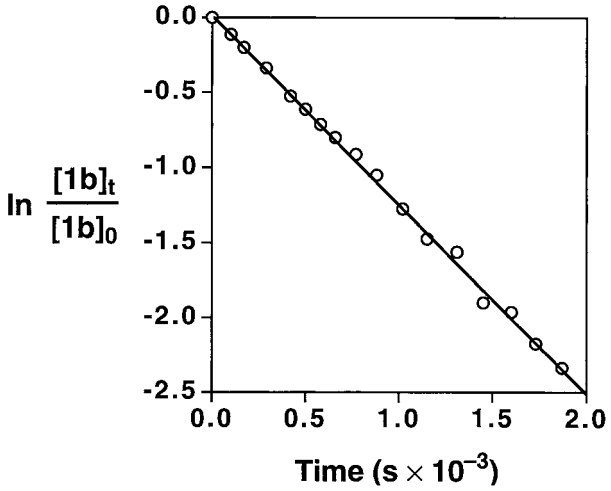

Figure 1. First-order plot for the thermal decomposition of **1b** at 23 °C in THF-d_8.

palladium-bound aryl group. For example, decomposition of *p*-nitrophenyl derivative **1d** at 23 °C was too fast to measure by ^{1}H NMR spectroscopy but occurred at a measurable rate at −1 °C ($t_{1/2}$ = 14 min). The *o*-nitrophenyl complex **1e** also decomposed readily at −1 °C ($t_{1/2}$ = 9 min). In contrast, decomposition of *p*-benzophenone complex **1c** was sluggish at 23 °C but occurred readily at 38 °C ($t_{1/2}$ = 8.6 min). Although *o*-cyanophenyl derivative **1f** decomposed slowly even at 62 °C ($t_{1/2}$ = 21 min), *o*-neopentoxybenzonitrile was generated in quantitative yield (99 ± 5%), without detectable formation of pivaldehyde. Overall, the rate of C−O reductive elimination decreased in the order *o*-NO_2 (**1e**) > *p*-NO_2 (**1d**) > *p*-CHO (**1b**) > *p*-COPh (**1c**) > *p*-CN (**1a**)[3] > *o*-CN (**1f**).[12]

In contrast to complexes **1a**−**f**, thermolysis of *p*-chlorophenyl derivative **1g** and the *m*-nitrophenyl and *m*-cyanophenyl derivatives **1h** and **1i** led to decomposition without formation of detectable quantities of aryl ether. Furthermore, thermolysis of **1g**−**i** produced kinetics consistent with auto-catalytic decomposition. For example, heating a solution of *p*-chlorophenyl complex **1g** at 47 °C in THF-d_8 led to no detectable decomposition (<5%) after 20 min. However, continued heating at 47 °C led to rapid decomposition over the following 20 min with formation of chlorobenzene in 40% yield (Figure 2). Significantly, no detectable quantities of *p*-neopentoxychlorobenzene or pivaldehyde were observed. Thermolysis of the *m*-nitrophenyl derivative **1h** and *m*-cyanophenyl complex **1i** led to analogous auto-catalytic decomposition with no detectable formation of aryl ether. The mechanisms of these auto-catalytic decomposition pathways were not investigated further.

We also investigated briefly the electronic dependence of C−O reductive elimination from dppf-ligated palladium neopentoxide complexes. In contrast to the BINAP derivatives **1a**−**f**, these complexes were susceptible to β-hydride elimination, leading to the formation of mixtures of aryl ether and pivaldehyde upon thermolysis. For example, we previously observed that *p*-cyanophenyl derivative (dppf)Pd(*p*-C_6H_4CN)(OCH_2CMe_3) (**2c**) decomposed at 55 °C with formation of *p*-neopentoxybenzonitrile (46%) and pivaldehyde (36%).[3] Substitution of *p*-cyanophenyl with a more electron-deficient aryl group led to dramatic rate acceleration and enhanced yields of aryl ether. For example, when a freshly prepared solution of the *p*-nitrophenyl complex **2a** was warmed from −50 to 23 °C, rapid decomposition occurred ($t_{1/2}$ = 7.1 min) with formation of *p*-neopentoxynitrobenzene (81%) and pivaldehyde (12%) (Scheme 5). In contrast, thermolysis of the *m*-cyanophenyl derivative **2b** formed pivaldehyde in 73% yield without generation of detectable quantities *m*-neopentoxybenzonitrile. The strong tendency of dppf palladium alkoxide complexes to undergo β-hydride elimination was also noted by Hartwig in a related study.[4b]

Discussion

Palladium-mediated C−O reductive elimination was facilitated by the presence of substituents on the palladium-bound aryl group suitable for the delocalization of negative charge, while simple electron-withdrawing groups failed to facilitate reductive elimination. For example, while reductive elimination occurred readily from the *p*-NO_2- (σ = 0.78) and *p*-CN (σ = 0.67) -substituted palladium aryl complexes **1d** and **1a**, the corresponding *m*-nitrophenyl (**1h**) and *m*-cyanophenyl derivatives (**1i**) were resistant toward C−O reductive elimination despite the significant σ values for *m*-NO_2 (σ = 0.71) and *m*-CN (σ = 0.56).[13] Likewise, despite the similar σ values for *p*-CHO (σ = 0.22) and *p*-Cl (σ = 0.23), *p*-benzaldehyde complex **1b** underwent reductive elimination readily at room temperature, while *p*-chlorophenyl derivative **1g** failed to undergo C−O reductive elimination upon extended thermolysis at 47 °C (Table 1). Consistent with this trend, the *o*-NO_2- and *o*-CN-substituted complexes **1e** and **1f** underwent C−O reductive elimination in quantitative yield.[12]

In an effort to quantify the relationship between rate of C−O reductive elimination and the degree of resonance stabilization of the palladium-bound aryl group, $\Delta G^{\ddagger}$ was plotted versus the parameter σ^- for the substituents on the palladium-bound aryl group (Figure 3).[14] Despite a fair amount of scatter due to the narrow range of σ^- values, a linear free energy relationship was observed between $\Delta G^{\ddagger}$ and σ^- where ρ = 6.4 ± 1.6.[15] It is noteworthy that this correlation parallels that observed in aromatic nucleophilic substitution, which is accelerated dramatically by the presence of resonance stabilizing groups.[16] For example, the rate of reaction of methoxide ion with para-substituted *o*-nitrochlorobenzene derivatives displayed a linear free energy relationship with σ^- where ρ = 3.90,[17] while the rate of reaction of methoxide ion with para-substituted chlo-

(11) In each case, formation of aryl ether was confirmed by ^{1}H NMR and GC analyses and comparison with authentic sample.

(12) Our previous results indicate that C−O reductive elimination from palladium BINAP and palladium Tol-BINAP complexes occurs with comparable rate and efficiency. For example, the rate of thermal decomposition of [BINAP]Pd(*p*-C_6H_4CN)(OCH_2CMe_3) at 47 °C was k_{obs} = 15.1 × 10^{-4} s^{-1} to form aryl ether in 87% yield (NMR).[2b] We were unable to isolate the complete series of palladium aryl halide derivatives with either BINAP or Tol-BINAP due to the wide range in solubility of the complexes as a function of phosphorous- and palladium-bound aryl groups.

(13) Ritchie, C. D.; Sager, W. F. *Prog. Phys. Org. Chem.* **1964**, *2*, 323.

(14) Lowry, T. H.; Richardson, K. S. *Mechanism and Theory in Organic Chemistry*, 3rd ed.; Harper and Row: New York, 1987; pp 149−151.

(15) Free energy was employed instead of ln *k* in an effort to compensate for the slightly different decomposition temperatures for the various compounds. The σ^- value for *p*-COPh was estimated from the σ^- value for *p*-COMe. Attempts to generate [BINAP]Pd(*p*-C_6H_4COMe)(OCH_2CMe_3) by treatment of [BINAP]Pd(*p*-C_6H_4COMe)(Br) with $KOCH_2CMe_3$ led to rapid decomposition without formation of the palladium (aryl)alkoxide complex. A plot of $\Delta G^{\ddagger}$ versus σ^- including only *p*-NO_2, *p*-CN, and *p*-CHO gave ρ = 8.4 ± 2.0.

(16) (a) Ehrenson, S.; Brownlee, R. T. C.; Taft, R. W. *Prog. Phys. Org. Chem.* **1973**, *10*, 1. (b) Wells, P. R.; Ehrenson, S.; Taft, R. W. *Prog. Phys. Org. Chem.* **1968**, *6*, 147.

(17) Miller, J. *J. Chem. Soc.* **1952**, 3550 (b) Miller, J. *Aust. J. Chem.* **1956**, *9*, 61. (c) Miller, J. *J. Am. Chem. Soc.* **1954**, *76*, 448. (d) Heppolette, R. L.; Miller, J. *J. Chem. Soc.* **1956**, 2329. (e) Miller, J.; Parker, A. J.; Bolto, B. A. *J. Am. Chem. Soc.* **1957**, *79*, 93. (f) Miller, J.; Parker, A. J. *Aust. J. Chem.* **1958**, *11*, 302. (g) Chan, T. L.; Miller, J.; Stansfield, F. *J. Chem. Soc.* **1964**, 1213.

Table 1. First-Order Rate Constants and Product Distribution for Thermal Decomposition of BINAP and Tol-BINAP Derivatives **1a−i** and **2a−c**

PdOR	Ar	σ^a	$\sigma^{-\,a}$	temp (°C)	k_{obs} ($s^{-1} \times 10^4$)[b]	$\Delta G^{\ddagger}$ (kcal mol^{-1})	yield ArOR (±5%)[c]	yield Me_3CHO (±5%)[c]
1a[d]	*p*-CN	0.66	0.90	47	15.3	22.9	85	<2
1b	*p*-CHO	0.22	1.13	23	12.6	21.4	95	<2
1c	*p*-COPh	0.50[e]	0.87[e]	38	13.5	22.2	98	<2
1d	*p*-NO_2	0.78	1.24	−1	8.18	19.8	102	<2
1e	*o*-NO_2			−1	12.2	19.6	103	<2
1f	*o*-CN			62	5.48	24.3	99	<2
1g	*p*-Cl	0.23		47	— —[f]		<2	24
1h	*m*-CN	0.56		62	— —[f]		<2	
1i	*m*-NO_2	0.71		47	— —[f]		<2	
2a	*p*-NO_2	0.78	1.24	23	16.2	21.2	81	12
2b	*m*-CN	0.56		47	13.5	23.0	<2	73
2c	*p*-CN	0.66	0.90	55	14.3	23.5	46	36

[a] Hammett values taken from ref 12. [b] See ref 12. [c] Determined by ^1H NMR spectroscopy. [d] Data taken from ref 2b. [e] σ and σ^- estimated from the respective values for *p*-COMe. [f] First-order kinetics not obeyed.

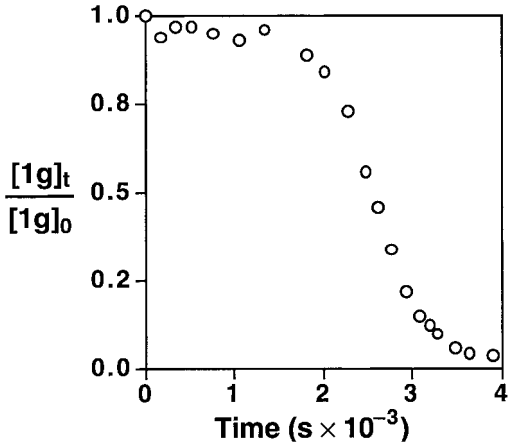

Figure 2. Plot of concentration versus time for the thermal decomposition of **1g** at 47 °C in THF-d_8.

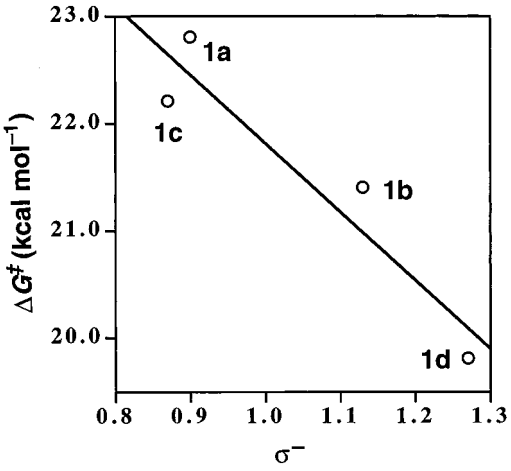

Figure 3. Plot of $\Delta G^{\ddagger}$ versus σ^- of the palladium-bound aryl substituent for thermolysis of complexes **1a−d**, where $\rho = 6.4 \pm 1.6$.

Scheme 5

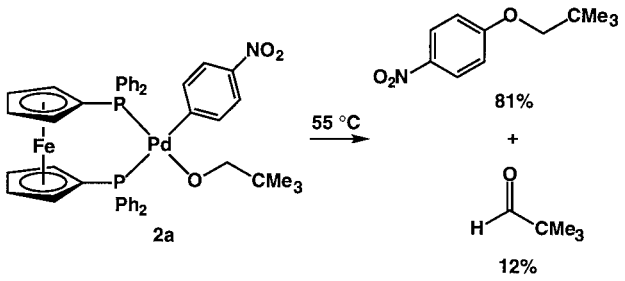

robenzenes displayed a linear free energy relationship with σ^- where $\rho = 8.47$.[18]

The close analogy between the electronic dependence of C−O reductive elimination and aromatic nucleophilic substitution points to the buildup of considerable negative charge in the palladium-bound aryl group in the transition state for C−O reductive elimination. We propose that the accumulation of negative charge in the palladium-bound aryl group in the transition state for C−O reductive elimination results from inner-sphere attack of the alkoxide oxygen atom at the ipso-carbon atom of the palladium-bound aryl group. For example, our kinetics are consistent with rapid and reversible generation of intermediate **I** followed by rate-limiting Pd−C heterolysis to form Pd[L−L] and aryl ether via a charge-separated transition state such as **II** (Scheme 6). Alternatively, our kinetics are consistent with rate-limiting alkoxide migration via a transition state such as **III** followed by rapid Pd−C bond cleavage. This concerted pathway is analogous to the insertion-type C−H[19] and C−C[20] reductive elimination pathways predicted by theoretical studies.

Although our data do not rule out a mechanism initiated by rapid and reversible alkoxide dissociation followed by outer-sphere attack of the alkoxide at the ipso-carbon atom, the proposed inner-sphere mechanism is in accord with the activation parameters determined for reductive elimination from **1a** [$\Delta H^{\ddagger} = 19.8 \pm 0.8$ kcal mol^{-1}, $\Delta S^{\ddagger} = -9.3 \pm 0.3$ eu][2b] and is supported by the proclivity of both CO[21] and isocyanides[22] to undergo α-migratory insertion into group 10 metal−alkoxide bonds. The high nucleophilicity of alkoxide ligands in late

(18) Miller, J.; Wan, K. Y. *J. Chem. Soc.* **1963**, 3492.

(19) Calhorda, M. J.; Brown, J. M.; Cooley, N. A. *Organometallics* **1991**, *10*, 1431.

(20) Silvestre, J.; Calhorda, M. J.; Hoffmann, R.; Stoutland, P. O.; Bergman, R. G. *Organometallics* **1986**, *5*, 1841.

(21) (a) Dockter, D. W.; Fanwick, P. E.; Kubiak, C. P. *J. Am. Chem. Soc.* **1996**, *118*, 4846. (b) Bryndza, H. E.; Calabrese, J. C.; Wreford, S. S.; *Organometallics* **1984**, *3*, 1603. (c) Bryndza, H. E.; Kretchmar, S. A.; Tulip, T. H. *J. Chem. Soc., Chem. Commun.* **1985**, 977. (d) Michelin, R. A.; Napoli, M.; Ros, R. *J. Organomet. Chem.* **1979**, *175*, 239. (e) Bennett, M. A.; Yoshida, T. *J. Am. Chem. Soc.* **1978**, *100*, 1750. (f) Arnold, D. P.; Bennett, M. A.; Crisp, G. T.; Jeffery, J. C. *Adv. Chem. Ser.* **1982**, *196*, 195. (g) Bennett, M. A. *J. Organomet. Chem.* **1986**, *300*, 7. (h) Bennett, M. A.; Rokicki, A. *Aust. J. Chem.* **1985**, *38*, 1307. (i) Appleton, T. G.; Bennett, M. A. *J. Organomet. Chem.* **1973**, *55*, C88. (j) Bennett, M. A. *J. Mol. Catal.* **1987**, *41*, 1. (k) Bennett, M. A.; Rokicki, A. *J. Organomet. Chem.* **1983**, *244*, C31. (l) Bennett, M. A.; Rokicki, A. J. *Organometallics* **1985**, *4*, 180. (m) Bryndza, H. E. *Organometallics* **1985**, *4*, 1686.

(22) Michelin, R. A.; Ros, R. *J. Organomet. Chem.* **1979**, *169*, C42.

Scheme 6

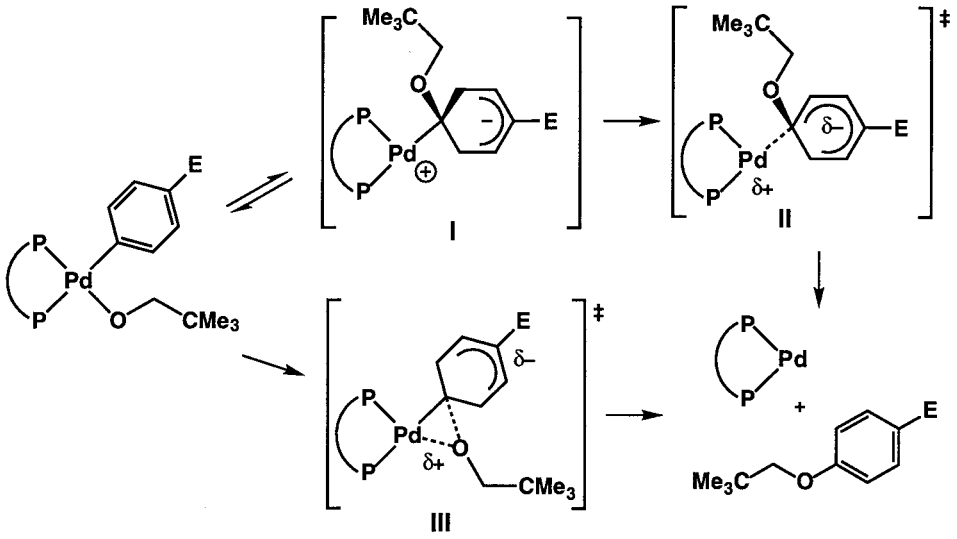

transition metal complexes has been documented[23] and is believed responsible for the higher rates of alkoxide migratory insertion relative to corresponding alkyl migratory insertion.[24] Likewise, migratory insertion of CO into a M−C bond displays electronic effects analogous to those observed for C−O reductive elimination. For example, addition of a Lewis acid such as $AlCl_3$ to a metal alkyl carbonyl complex often leads to dramatic (10^8) increase in the rate of CO migratory insertion due to polarization of the carbonyl C−O bond.[25]

The electronic dependence of C−O reductive elimination differs markedly from that of C−C reductive elimination but displays similarities with both C−S and C−N reductive elimination.[5,27] For example, both experiment[27,28] and theory[29] indicate that the rate of C−C reductive elimination increases with the increasing σ-donating ability of the eliminating ligands. In contrast, both C−S[5a] reductive elimination from palladium (aryl)thiolate complexes and C−N[5b,26] reductive elimination from palladium (aryl)amido complexes were accelerated by the presence of electron-withdrawing groups on the palladium-bound aryl group. In both cases, the rates did not correspond linearly to the σ values of the respective para-substituents, but were dependent on both inductive (σ) and resonance (σ^-) effects. In addition, the rate of C−N elimination increased with the increasing nucleophilicity of the respective amide, consistent with reductive elimination proceeding to some degree via an intramolecular nucleophile/electrophile pathway. However, in contrast to these C−X reductive eliminations, the rate of C−O reductive elimination from palladium (aryl)alkoxide complexes depends predominantly on resonance effects and to little extent on inductive effects.

The proposed insertion mechanism does not appear to be the only one available for C−O reductive elimination. For example, *intramolecular* C−O reductive elimination occurs readily under both catalytic[2a] and stoichiometric[2b] conditions from palladium complexes which do not possess resonance-stabilizing groups on the palladium-bound aryl group. Similarly, we have previously observed catalytic cross-coupling of *p-tert*-butylbenzene and sodium *tert*-butoxide in the presence of mixtures of $Pd_2(dba)_3$ (dba = *trans,trans*-dibenzylideneacetone) and Tol-BINAP. These results indicate the availability, at least in some instances, of energetically accessible alternative pathways for the reductive elimination process to form C−O bonds.

Conclusions

C−O reductive elimination from palladium (aryl)neopentoxide complexes was facilitated by the presence of substituents on the palladium-bound aryl group capable of delocalizing negative charge. The rate data displayed a scattered yet linear free energy relationship with σ^-, generating a ρ value comparable to that observed for uncatalyzed aromatic nucleophilic aromatic substitution. These observations are consistent with the buildup of negative charge in the palladium-bound aryl group in the transition state for C−O reductive elimination. This charge accumulation can be accounted for by a mechanism initiated by inner-sphere nucleophilic attack of the alkoxide ligand at the ipso-carbon atom of the palladium-bound aryl group to form a zwitterionic Meisenheimer intermediate or transition state. Significantly, both the electronic dependence and mechanism of C−O reductive elimination differs markedly from that of C−C reductive elimination. However, the proposed mechanism does not appear to be the only mechanism available for C−O reductive elimination.

Experimental Section

General Methods. All manipulations and reactions were performed under an atmosphere of nitrogen or argon in a glovebox or by standard Schlenk techniques. NMR spectra were recorded on a Varian XL-300

(23) (a) Kegley, S. E.; Schaverien, C. J.; Freudenberger, J. H.; Bergman, R. G.; Nolan, S. P.; Hoff, C. D. *J. Am. Chem. Soc.* **1987**, *109*, 6563. (b) Osakada, K.; Kim, Y. J.; Yamamoto, A. *J. Organomet. Chem.* **1990**, *382*, 303. (c) Kim, Y. J.; Osakada, K.; Takenaka, A.; Yamamoto, A. *J. Am. Chem. Soc.* **1990**, *112*, 1096. (d) Osakada, K.; Kim, Y. J.; Tanaka, M.; Ishiguro, S.; Yamamoto, A. *Inorg. Chem.* **1991**, *30*, 197. (e) Shubina, E. S.; Belkova, N. V.; Krylov, A. N.; Vorontsov, E. V.; Epstein, L. M.; Gusev, D. G.; Niedermann, M.; Berke, H. *J. Am. Chem. Soc.* **1996**, *118*, 1105.

(24) Bryndza, H. E.; Tam, W. *Chem. Rev.* **1988**, *88*, 1163.

(25) (a) McLain, S. J. *J. Am. Chem. Soc.* **1983**, *105*, 6355. (b) Labinger, J. A.; Bonfiglio, J. N.; Grimmet, D. L.; Masuo, S. T.; Shearin, E.; Miller, J. S. *Organometallics* **1983**, *2*, 733. (c) Grimmett, D. L.; Labinger, J. A.; Bonfiglio, J. N.; Masuo, S. T.; Shearin, E.; Miller, J. S. *Organometallics* **1983**, *2*, 1325. (d) Butts, S. B.; Richmond, T. G.; Shriver, D. F. *Inorg. Chem.* **1981**, *20*, 278. (e) Grundy, K. R.; Roper, W. R. *J. Organomet. Chem.* **1981**, *216*, 255. (f) Butts, S. B.; Straus, S. H.; Holt, E. M.; Stimson, R. E.; Alcock, N. W.; Shriver, D. F. *J. Am. Chem. Soc.* **1980**, *102*, 5093. (g) Richmond, T. G.; Basolo, F.; Shriver, D. F. *Inorg. Chem.* **1982**, *21*, 1272.

(26) Hartwig, J. F.; Richards, S.; Barañano, D.; Paul, F. *J. Am. Chem. Soc.* **1996**, *118*, 3626.

(27) Milstein, D.; Stille, J. K. *J. Am. Chem. Soc.* **1979**, *101*, 4981.

(28) Komiya, S.; Abe, Y.; Yamamoto, A.; Yamamoto, T. *Organometallics* **1983**, *2*, 1466.

(29) Tatsumi, K.; Hoffmann, R.; Yamamoto, A.; Stille, J. *Bull. Chem. Soc. Jpn.* **1981**, *54*, 7.

spectrometer at 23 °C unless otherwise noted. Gas chromatography was performed on a Hewlett-Packard model 5890 gas chromatograph using a 25 m poly(dimethylsiloxane) capillary column. Elemental analyses were performed by E+R Microanalytical Laboratories (Corona, NY). Diethyl ether, hexane, and THF-d_8 were distilled from solutions of sodium/benzophenone ketyl under argon or nitrogen. $Pd_2(dba)_3$, P(*o*-tolyl)$_3$, (*R*)-Tol-BINAP, (*S*)-BINAP, dppf (Strem), aryl halides (Aldrich), and DMF (Aldrich, anhydrous) were used as received. $KOCH_2CMe_3$ was synthesized from reaction of anhydrous neopentanol (Aldrich) and 1 equiv of KH in THF.

Palladium (Aryl)halide Dimers. Palladium (aryl)halide dimers were prepared from $Pd_2(DBA)_3$ (1.0 g, 1.1 mmol), P(*o*-tolyl)$_3$ (1.3 g, 4.3 mmol), and aryl halide (1.75 g) in benzene (60 mL) at room-temperature employing procedures analogous to published protocols.[30]

{Pd[P(*o*-tolyl)$_3$](*p*-C$_6$H$_4$NO$_2$)(*μ*-I)}$_2$. Tan solid (79%). Anal. Calcd (found) for $C_{54}H_{50}I_2N_2O_4P_2Pd_2$: C, 49.15 (48.93); H, 3.82 (4.02).

{Pd[P(*o*-tolyl)$_3$](*o*-C$_6$H$_4$NO$_2$)(*μ*-I)}$_2$. Brown solid (62%). Anal. Calcd (found) for $C_{54}H_{50}I_2N_2O_4P_2Pd_2$: C, 49.15 (49.37); H, 3.82 (3.98).

{Pd[P(*o*-tolyl)$_3$](*m*-C$_6$H$_4$NO$_2$)(*μ*-I)}$_2$. Tan solid (77%). Anal. Calcd (found) for $C_{54}H_{50}I_2N_2O_4P_2Pd_2$: C, 49.15 (49.26); H, 3.82 (3.85).

{Pd[P(*o*-tolyl)$_3$](*p*-C$_6$H$_4$Cl)(*μ*-Br)}$_2$. Bright yellow solid (71%). Anal. Calcd (found) for $C_{54}H_{50}Br_2Cl_2P_2Pd_2$: C, 53.85 (54.04); H, 4.18 (4.44).

{Pd[P(*o*-tolyl)$_3$](*m*-C$_6$H$_4$CN)(*μ*-Br)}$_2$. Yellow powder (67%). Anal. Calcd (found) for $C_{56}H_{50}Br_2O_2P_2Pd_2$: C, 56.73 (56.79); H, 4.25 (4.27).

{Pd[P(*o*-tolyl)$_3$](*o*-C$_6$H$_4$CN)(*μ*-Br)}$_2$. Yellow powder (72%). Anal. Calcd (found) for $C_{56}H_{50}Br_2O_2P_2Pd_2$: C, 56.73 (56.98); H, 4.25 (4.55).

{Pd[P(*o*-tolyl)$_3$](*p*-C$_6$H$_4$COPh)(*μ*-Br)}$_2$. Cream-colored solid (53%). Anal. Calcd (found) for $C_{68}H_{60}Br_2O_2P_2Pd_2$: C, 60.78 (61.00); H, 4.50 (4.75).

{Pd[P(*o*-tolyl)$_3$](*p*-C$_6$H$_4$CHO)(*μ*-Br)}$_2$. Bright yellow solid (64%). Anal. Calcd (found) for $C_{56}H_{52}Br_2O_2P_2Pd_2$: C, 56.45 (56.75); H, 4.40 (4.43).

Palladium (Aryl)halide Monomers. Palladium (aryl)halide monomers were prepared from the respective palladium (aryl)halide dimer (200 mg, 0.30 mmol), BINAP (220 mg, 0.35 mmol), Tol-BINAP (240 mg, 0.35 mmol), or dppf (200 mg, 0.36 mmol) employing procedures analogous to published protocols,[2b] unless otherwise noted.

[(±)-BINAP]Pd(*p*-C$_6$H$_4$CHO)(Br). Pale yellow microcrystals from ether (84%). ^{1}H NMR (THF-d_8): δ 9.71 (s, 1 H), 8.02 (t, J = 9.1 Hz), 7.82 (m, 3 H), 7.70−7.55 (m, 6 H), 7.45 (br s, 5 H), 7.42−7.31 (m, 3 H), 7.25−7.15 (m, 3 H), 7.12−6.90 (m, 8 H), 6.78−6.50 (m, 7 H). ^{31}P{^{1}H}NMR: δ 27.6 (d, J = 38.3 Hz), 12.6 (d, J = 38.9 Hz). Anal. Calcd (found) for $C_{51}H_{37}BrOP_2Pd$: C, 67.01 (67.18); H, 4.08 (4.17).

[(*S*)-BINAP]Pd(*p*-C$_6$H$_4$COPh)(Br). White solid from ether (73%). ^{1}H NMR (THF-d_8): δ 8.03 (t, J = 8.7 Hz, 1 H), 7.88−7.78 (m, 3 H), 7.70−7.50 (m, 19 H), 7.17 (t, J = 8.6 Hz, 6 H), 7.01 (t, J = 7.4 Hz, 5 H), 6.80−6.50 (m, 9 H). ^{31}P{^{1}H}NMR: δ 27.9 (d, J = 38.6 Hz), 12.4 (d, J = 38.7 Hz). Anal. Calcd (found) for $C_{57}H_{41}BrOP_2Pd$: C, 69.14 (69.10); H, 4.17 (3.99).

[(*R*)-Tol-BINAP]Pd(*p*-C$_6$H$_4$NO$_2$)(I). Tan solid from hexane/ether (62%) which contained traces of hexane (<5% by ^{1}H NMR). ^{1}H NMR (THF-d_8): δ 8.01 (t, J = 8.0 Hz, 1 H), 7.84 (d, J = 7.1 Hz, 1 H), 7.66 (m), 7.55 (m), 7.38 (t, J = 8.3 Hz), 7.29 (d, J = 6.7 Hz), 7.13 (t, J = 8.3 Hz, 2 H), 6.94 (m), 6.81 (d, J = 6.3 Hz, 2 H), 6.54 (d, J = 8.4 Hz, 1 H), 6.45 (d, J = 7.2 Hz, 2 H), 6.33 (d, J = 6.7 Hz, 2 H), 2.42 (s, 3 H), 2.15 (s, 3 H), 1.96 (s, 3 H), 1.95 (s, 3 H). ^{31}P{^{1}H}NMR (THF-d_8): δ 26.3 (d, J = 37.8 Hz), 11.7 (d, J = 37.8 Hz). Anal. Calcd (found) for $C_{54}H_{44}INO_2P_2Pd$: C, 62.71 (62.97); H, 4.29 (4.28).

[(*R*)-Tol-BINAP]Pd(*m*-C$_6$H$_4$NO$_2$)(I)·CH$_2$Cl$_2$. Brown blocks from CH_2Cl_2/hexane (37%). ^{1}H NMR (THF-d_8): δ 8.13 (d, J = 8 Hz, 1 H), 7.99 (t, J = 9.5 Hz, 1 H), 7.79 (d, J = 8.4 HZ, 1 H), 7.74−7.20 (m, 16 H), 7.09−6.93 (m, 4 H), 6.83−6.76 (m, 4 H), 6.54 (d, J = 8.5 Hz, 1 H), 6.44 (d, J = 7.3 Hz, 2 H), 6.36 (d, J = 7.1 Hz, 2 H), 2.40 (s, 3 H), 2.14 (s, 3 H), 1.96 (s, 3 H), 1.94 (s, 3 H). ^{31}P{^{1}H}NMR ($CDCl_3$): δ 21.5 (d, J = 38.7 Hz), 10.1 (d, J = 38.6 Hz). Anal. Calcd (found) for $C_{55}H_{46}Cl_2INO_2P_2Pd$: C, 59.03 (58.15); H, 4.14 (4.23).

[(±)-BINAP]Pd(*o*-C$_6$H$_4$NO$_2$)(I). Brown needles from Et_2O (81%). ^{1}H NMR (THF-d_8): δ 8.20−6.40 (m, 36 H) (resonances corresponding to a 3:2 ratio of isomers were observed). ^{31}P{^{1}H}NMR (THF-d_8): δ 19.4 (d, J = 38.5 Hz), 12.6 (d, J = 38.6 Hz) [major isomer]; δ 17.8 (d, J = 40.1 Hz), 14.8 (d, J = 40.0 Hz) [minor isomer]. Anal. Calcd (found) for $C_{51}H_{36}INO_2P_2Pd$: C, 61.87 (61.88); H, 3.66 (3.77).

[(*R*)-Tol-BINAP]Pd(*m*-C$_6$H$_4$CN)(Br). Cream-colored microcrystals from ether (84%). ^{1}H NMR (THF-d_8): δ 7.96 (t, J = 9.6 Hz, 1 H), 7.82−7.58 (m, 7 H), 7.50−7.24 (m, 9 H), 7.16−6.94 (m, 7 H), 6.92−6.70 (m, 4 H), 6.57 (d, J = 8.7 Hz, 1 H), 6.45 (d, J = 7.5 Hz, 2 H), 6.35 (d, J = 6.9 Hz, 2 H). ^{31}P{^{1}H}NMR (THF-d_8): δ 23.1 (d, J = 38.1 Hz), 8.6 (d, J = 37.7 Hz). Anal. Calcd (found) for $C_{55}H_{44}BrNP_2Pd$: C, 68.30 (68.11); H, 4.59 (4.82).

[(*S*)-Tol-BINAP]Pd(*o*-C$_6$H$_4$CN)(Br). Cream-colored solid from ether (74%). ^{1}H NMR (THF-d_8): in addition to aromatic resonances at δ 8.50−6.40 (m, 36 H), resonances corresponding to a 2:1 mixture of isomers were observed at δ 2.42 (s, 3 H), 1.95 (s, 3 H), 1.89 (s, 3 H), 2.12 (s, 3 H) [major isomer]; 2.40 (s, 3 H), 2.14 (s, 3 H), 1.97 (s, 3 H), 1.91 (s, 3 H) [minor isomer]. ^{31}P{^{1}H}NMR (THF-d_8): δ 26.2 (d, J = 34.8 Hz), 11.1 (d, J = 34.6 Hz) [major isomer]; 24.6 (d, J = 35.9 Hz), 13.3 (d, J = 36.2 Hz) [minor isomer]. Anal. Calcd (found) for $C_{55}H_{44}BrNP_2Pd$: C, 68.30 (68.57); H, 4.59 (4.80).

[(*S*)-BINAP]Pd(*p*-C$_6$H$_4$Cl)(Br). Yellow microcrystals from ether (81%), which contained traces of ether (<5% by ^{1}H NMR). ^{1}H NMR (THF-d_8): δ 7.97 (t, J = 8.7 Hz, 1 H), 7.86−7.76 (m, 3 H), 7.66−7.56 (m, 4 H), 7.50−7.30 (m, 9 H), 7.20−6.94 (m, 9 H), 6.80−6.50 (m, 8 H). ^{31}P {^{1}H} NMR: δ 27.9 (d, J = 38.3 Hz), 12.5 (d, J = 38.1 Hz). Anal. Calcd (found) for $C_{50}H_{36}BrClP_2Pd$: C, 65.24 (65.23); H, 3.94 (4.03).

(dppf)Pd(*p*-C$_6$H$_4$NO$_2$)(Br). Bright yellow solid (94%). ^{1}H NMR ($CDCl_3$, 23 °C): δ 8.02 (m, 4 H), 7.48 (s, 6 H), 7.40−7.26 (m, 6 H), 7.19 (br t, J = 7.5 Hz, 6 H), 7.10 (dt, J = 7.2, 2.33 Hz, 6 H), 4.70 (d, J = 2.2 Hz, 2 H), 4.52 (s, 2 H), 4.16, (s, 2 H), 3.60 (d, J = 2.3 Hz, 2 H). ^{31}P {^{1}H} NMR ($CDCl_3$): δ 30.8 (d, J = 31.1 Hz), 10.8 (d, J = 31.1 Hz). Anal. Calcd (found) for $C_{40}H_{32}BrNFeO_2P_2Pd$: C, 55.68 (55.76); H, 3.74 (3.83).

(dppf)Pd(*m*-C$_6$H$_4$CN)(Br). Bright yellow powder (90%). ^{1}H NMR (THF-d_8): δ 8.00 (br s, 4 H), 7.48 (s, 8 H), 7.40−7.00 (m, 10 H), 6.77 (d, J = 7.7 Hz, 1 H), 6.63 (d, J = 7.6 Hz, 1 H), 4.77 (s, 1 H), 4.63 (s, 1 H), 4.54 (s, 1 H), 4.49 (s, 1 H), 4.15 (s, 2 H), 3.58 (br s, 2 H). ^{31}P{^{1}H}NMR (THF-d_8): δ 31.3 (d, J = 31.0 Hz), 10.7 (d, J = 31.2 Hz). Anal. Calcd (found) for $C_{41}H_{32}BrFeNP_2Pd$: C, 58.43 (58.71); H, 3.83 (3.84).

Palladium (Aryl)neopentoxide Complexes. Palladium (aryl)-neopentoxide complexes were generated in solution by addition of 1 equiv of a $KOCH_2CMe_3$ solution in THF-d_8 to a THF-d_8 solution (∼15 mM) of the appropriate palladium halide complex unless otherwise noted.[2b]

[(±)-BINAP]Pd(*p*-C$_6$H$_4$CHO)(OCH$_2$CMe$_3$) (1b). ^{1}H NMR (THF-d_8, −52 °C): δ 9.70 (s, 1 H), 7.93 (t, J = 9.6 Hz), 7.8−7.65 (m), 7.63 (t, J = 8.7 Hz), 7.45 (br s), 7.30 (br s), 7.20−7.00 (m), 6.95−6.52 (m), 6.51 (br s), 2.79 (d, J = 8.3 Hz, 1 H), 2.61 (d, J = 8.3 Hz, 1 H), 0.11, (s, 9 H). ^{31}P{^{1}H}NMR (THF-d_8, −55 °C): δ 31.8 (d, J = 36.8 Hz), 14.7 (d, J = 36.8 Hz).

[(*S*)-BINAP]Pd(*p*-C$_6$H$_4$COPh)(OCH$_2$CMe$_3$) (1c). ^{1}H NMR (THF-d_8, −52 °C): δ 7.94 (t, J = 9.0 Hz, 3 H), 7.78−6.95 (m, 30 H), 6.80−6.50 (m, 8 H), 2.90 (d, J = 8.5 Hz, 1 H) 2.73 (d, J = 8.4 Hz, 1 H), 0.19 (s, 9 H). ^{31}P{^{1}H}NMR (THF-d_8, −55 °C): δ 32.0 (d, J = 36.7 Hz), 14.6 (d, J = 36.8 Hz).

[(*R*)-Tol-BINAP]Pd(*p*-C$_6$H$_4$NO$_2$)(OCH$_2$CMe$_3$) (1d). ^{1}H NMR (THF-d_8, −54 °C): δ 7.80−6.70 (m, 36 H), 2.75 (d, J = 8.0 Hz, 1 H), 2.66 (d, J = 8.3 Hz, 1 H), 2.39 (s, 3 H), 2.14 (s, 3 H), 1.98 (s, 3 H), 1.96 (s, 3 H), 0.13 (s, 9 H). ^{31}P{^{1}H}NMR (THF-d_8, −55 °C): δ 33.4 (d, J = 36.7 Hz), 17.2 (d, J = 36.7 Hz).

[(±)-BINAP]Pd(*o*-C$_6$H$_4$NO$_2$)(OCH$_2$CMe$_3$) (1e). ^{1}H NMR (THF-d_8, −55 °C): (a ∼10:1 ratio of isomers was observed; peaks corresponding to the major isomer are reported) δ 8.92 (m, 1 H), 8.46 (m, 1 H), 8.12−6.45 (m, 34 H), 2.60 (d, J = 8.3 Hz, 1 H), 2.33 (d, J = 8.3 Hz, 1 H), 0.04 (s, 9 H). ^{31}P{^{1}H}NMR (THF-d_8, −55 °C): δ 29.7 (d, J = 38.9 Hz), 18.4 (d, J = 38.7 Hz).

(30) Widenhoefer, R. A.; Zhong, H. A.; Buchwald, S. L. *Organometallics* **1996**, *15*, 2745.

[(*S*)-Tol-BINAP]Pd(*o*-C_6H_4CN)(OCH_2CMe_3) (1f). ^{1}H NMR (23 °C, THF-d_8): (in addition to aromatic resonances at δ 9.01 (m), 8.40−6.20 (m), and 5.60 (m), peaks corresponding to a 1:2 ratio of isomers were observed) 2.69 (d, J = 8.4 Hz, 1 H), 2.61 (d, J = 9.1 Hz, 1 H), 2.39 (s, 3 H), 2.13 (s, 3 H), 1.97 (s, 3 H), 1.87 (s, 3 H), 0.09 (s, 9 H) [major isomer]; 2.81 (br d, J = 8.6 Hz, 1 H), 2.57 (d, J = 8.8 Hz, 1 H), 0.09 (s, 9 H) [minor isomer]. ^{31}P{^{1}H}NMR (THF-d_8): δ 30.0 (d, J = 36.7 Hz), 14.7 (d, J = 35.4 Hz) [major isomer]; 28.3 (d, J = 36.0 Hz), 17.4 (d, J = 37.2 Hz) [minor isomer].

[(*S*)-BINAP]Pd(*p*-C_6H_4Cl)(OCH_2CMe_3) (1g). ^{1}H NMR (23 °C, THF-d_8): δ 8.0−6.5 (m, 36 H), 2.85 (d, J = 8.6 Hz, 1 H), 2.67 (d, J = 8.0 Hz, 1 H), 0.18 (s, 9 H). ^{31}P {^{1}H} NMR (THF-d_8, 23 °C): δ 30.4 (d, J = 36.4 Hz), 14.1 (d, J = 36.3 Hz).

[(*R*)-Tol-BINAP]Pd(*m*-$C_6H_4NO_2$)(OCH_2CMe_3) (1h). ^{1}H NMR (23 °C, THF-d_8): δ 8.20 (d, J = 7.3 Hz, 1 H), 7.90−7.20 (m, 17 H), 7.06 (m, 5 H), 6.81 (m, 4 H), 6.72 (d, J = 8.6 Hz, 1 H), 6.45 (d, J = 7.3 Hz, 2 H), 6.35 (d, J = 7.3 Hz, 2 H), 2.80 (d, J = 8.3 Hz, 1 H), 2.67 (d, J = 8.4 Hz, 1 H), 2.37 (s, 3 H), 2.14 (s, 3 H), 1.98 (s, 3 H), 1.94 (s, 3 H), 0.19 (s, 9 H). ^{31}P{^{1}H}NMR (THF-d_8, 23 °C): δ 29.6 (d, J = 37.2 Hz), 13.8 (d, J = 37.3 Hz).

[(*R*)-Tol-BINAP]Pd(*m*-C_6H_4CN)(OCH_2CMe_3) (1i). A suspension of Pd[(*R*)-Tol-BINAP](*m*-C_6H_4CN)Br (100 mg, 0.103 mmol) and potassium neopentoxide (13 mg, 0.103 mmol) in Et_2O (7 mL) was stirred at room temperature for 5 min. The resulting orange suspension was filtered through Celite, concentrated to ∼1 mL under vacuum, and diluted with hexane (10 mL). The precipitate which formed over 2 h was collected, washed with pentane, and dried under vacuum to give **1i** (72 mg, 72%) as yellow microcrystals. ^{1}H NMR (THF-d_8): δ 7.84−7.22 (m, 17 H), 7.18−6.64 (m, 11 H), 6.45 (d, J = 7.3 Hz, 2 H), 6.33 (d, J = 7.3 Hz, 2 H), 2.78 (d, J = 8.6 Hz, 1 H), 2.65 (d, J = 8.6 Hz, 1 H), 2.38 (s, 3 H), 2.20 (s, 3 H), 1.98 (s, 3 H), 1.95 (s, 3 H), 0.20 (s, 9 H). ^{31}P{^{1}H}NMR (THF-d_8): δ 29.6 (d, J = 36.8 Hz), 13.7 (d, J = 36.7 Hz). Anal. Calcd (found) for $C_{60}H_{55}NOP_2Pd$: C, 73.69 (73.66); H, 5.69 (5.97).

(dppf)Pd(*p*-$C_6H_4NO_2$)(OCH_2CMe_2) (2a). ^{1}H NMR (23 °C, THF-d_8): δ 8.21 (m, 4 H), 7.50−7.00 (m, 20 H), 4.86 (s, 2 H), 4.59 (s, 2 H), 4.21 (s, 2 H), 3.56 (s, 2 H, Cp), 2.70 (s, 2 H), 0.26 (s, 9 H). ^{31}P-{^{1}H}NMR (THF-d_8, 23 °C): δ 30.3 (d, J = 31.8 Hz), 11.8 (d, J = 31.9 Hz).

(dppf)Pd(*m*-C_6H_4CN)(OCH_2CMe_3) (2b): ^{1}H NMR (23 °C, THF-d_8): δ 8.21 (m, 4 H), 7.50−7.10 (m, 18 H), 6.79−6.63 (m, 2 H), 4.84 (s, 2 H), 4.58 (s, 2 H), 4.20 (s, 2 H), 3.55 (s, 2 H) 2.66 (s, 2 H), 0.22 (s, 9 H). ^{31}P{^{1}H} NMR (THF-d_8, 23 °C): δ 32.4 (d, J = 31.4 Hz), 13.2 (d, J = 31.7 Hz).

Aryl Neopentyl Ethers. *o*-$CNC_6H_4OCH_2CMe_3$. A mixture of 2-bromobenzonitrile (500 mg, 2.73 mmol), neopentanol (289 mg, 3.3 mmol), and sodium hydride (131 mg, 5.5 mmol) in DMF (10 mL) was stirred at 80 °C for 30 min. After the resulting dark brown suspension was cooled to room temperature, ether (20 mL) and water (20 mL) were added and the layers were separated. The aqueous layer was extracted with Et_2O (3 × 20 mL), and the combined organic layers were washed with brine (30 mL), dried ($MgSO_4$), and concentrated using a rotary evaporator. The yellow residue was chromatographed [SiO_2; hexanes:EtOAc (12:1)]. The first band to elute was collected and concentrated under vacuum to give *o*-$CNC_6H_4OCH_2CMe_3$ (199 mg, 31%) as a colorless oil which solidified on standing. ^{1}H NMR (THF-d_8): δ 7.60−7.52 (m, 2 H), 7.11 (d, J = 8.6 Hz, 1 H), 7.01 (t, J = 7.6 Hz, 1 H), 3.77 (s, 2 H), 1.05 (s, 9 H). ^{13}C{^{1}H}NMR (THF-d_8): δ 162.1, 135.1, 134.5, 121.6, 116.6, 113.6, 103.4, 79.5, 32.8, 27.0. IR (neat, cm^{-1}): 2960, 2223, 1598, 1478, 1478, 1402, 1364, 1297, 1260, 1164, 112, 1048, 1012, 842, 746. Anal. Calcd (found) for $C_{12}H_{15}NO$: C, 76.16 (76.29); H, 7.99 (8.18).

***p*-$NO_2C_6H_4OCH_2CMe_3$.**[31] Reaction of 4-fluoronitrobenzene (514 mg, 3.65 mmol), neopentanol (385 mg, 4.38 mmol), and NaH (175 mg, 7.29 mmol) in DMF (15 mL) at room temperature for 15 min followed by work up gave *p*-$NO_2C_6H_4OCH_2CMe_3$ (582 mg, 77%) as a pale yellow oil which solidified on standing. ^{1}H NMR (THF-d_8) δ 8.19 (d, J = 9.2 Hz, 2 H), 7.07 (d, J = 9.3 Hz, 2 H), 3.77 (s, 2 H), 1.07 (s, 9 H). ^{13}C{^{1}H}NMR (THF-d_8): δ 165.5, 142.5, 126.4, 114.4, 79.2, 32.5, 26.7. IR (neat, cm^{-1}): 2960, 2871, 1607, 1514, 1366, 1336, 1260, 1173, 1111, 1041, 1006, 947, 752, 691. Anal. Calcd (found) for $C_{11}H_{15}NO_3$: C, 63.14 (63.20); H, 7.23 (7.15).

***o*-$NO_2C_6H_4OCH_2CMe_3$.** Reaction of 2-fluoronitrobenzene (510 mg, 3.62 mmol), neopentanol (375 mg, 4.26 mmol), and NaH (175 mg, 7.29 mmol) in DMF (15 mL) at room temperature for 15 min followed by work up gave *o*-$NO_2C_6H_4OCH_2CMe_3$ (621 mg, 82%) as a yellow oil. ^{1}H NMR (THF-d_8) δ 7.81 (d, J = 8.9 Hz, 1 H), 7.53 (t, J = 7.9 Hz, 1 H), 7.21 (d, J = 8.4 Hz, 1 H), 7.02 (t, J = 7.7 Hz, 1 H), 3.78 (s, 2 H), 1.06 (s, 9 H). ^{13}C{^{1}H}NMR (THF-d_8): δ 153.5, 134.7, 126.0, 125.9, 120.8, 115.3, 79.7, 32.7, 26.8. IR (neat, cm^{-1}): 2961, 1609, 1526, 1352, 1287, 1257, 1010, 745. Anal. Calcd (found) for $C_{11}H_{15}NO_3$: C, 63.14 (63.41); H, 7.23 (7.42).

***p*-$PhC(O)C_6H_4OCH_2CMe_3$.** Reaction of 4-fluorobenzophenone (712 mg, 3.56 mmol), neopentanol (385 mg, 4.38 mmol), and NaH (175 mg, 7.29 mmol) in DMF (15 mL) at room temperature overnight followed by work up gave *p*-$COPhC_6H_4OCH_2CMe_3$ (470 mg, 49%) as a viscous, colorless oil. ^{1}H NMR (THF-d_8): δ 8.19 (d, J = 9.2 Hz, 2 H), 7.07 (d, J = 9.3 Hz, 2 H), 3.77 (s, 2 H), 1.07 (s, 9 H). ^{13}C{^{1}H}-NMR (THF-d_8): δ 194.6, 164.1, 139.7, 133.0, 132.4, 131.1, 130.4, 129.0, 114.8, 78.7, 32.5, 26.8. IR (neat, cm^{-1}): 2942, 1654, 1601, 1508, 1477, 1317, 1281, 1247, 1171, 1149, 1047, 1016, 923, 849, 741, 637, 625. Anal. Calcd (found) for $C_{18}H_{20}O_2$: C, 80.56 (80.36); H, 7.51, (7.55).

***p*-$CNC_6H_4OCH_2CMe_3$.** Reaction of 4-bromobenzonitrile (1.33 g, 7.27 mmol), neopentanol (750 mg, 8.52 mmol), and NaH (350 mg, 14.6 mmol) in DMF (30 mL) at 80 °C for 2 h followed by work up gave *p*-$CNC_6H_4OCH_2CMe_3$ (982 mg, 71%) as a colorless oil. ^{1}H NMR (THF-d_8): δ 7.61 (d, J = 8.1 Hz, 2 H), 7.04 (d, J = 8.1 Hz, 2 H), 3.70 (s, 2 H), 1.05 (s, 9 H). ^{13}C{^{1}H}NMR (THF-d_8): δ 163.7, 134.7, 119.4, 116.1, 105.1, 78.8, 32.5, 26.7. IR (neat, cm^{-1}): 2958, 2225, 1607, 1510, 1477, 1304, 1255, 1171, 1045, 1013, 835. Anal. Calcd (found) for $C_{12}H_{15}NO$: C, 76.16 (76.35); H, 7.99 (7.86).

***p*-$HC(O)C_6H_4OCH_2CMe_3$.** *p*-Neopentoxybenzaldehyde was formed via reduction of *p*-neopentoxybenzonitrile employing a procedure analogous to known protocols.[32] DIBAL (1.05 mL, 1.5 M, 1.58 mmol) was added dropwise to a solution of *p*-$CNC_6H_4OCH_2CMe_3$ (262 mg, 1.38 mmol) in Et_2O (10 mL) at −78 °C. The solution was stirred at −78 °C for 30 min and then warmed to room temperature and stirred for 1 h. After the reaction was quenched by addition of water (1 mL) at 0 °C, 1 N HCl (25 mL) and ether (25 mL) were added, and the resulting mixture was stirred vigorously for 15 min. The layers were separated, and the aqueous phase was extracted with ether (3 × 20 mL). The combined organic fractions were dried ($MgSO_4$), concentrated, and chromatographed (SiO_2; hexane:EtOAc (12:1) to give *p*-$CHOC_6H_4OCH_2CMe_3$ (152 mg, 58%) as a colorless oil. ^{1}H NMR (THF-d_8): δ 9.85 (s, 1 H), 7.81 (d, J = 8.5 Hz, 2 H), 7.06 (d, J = 8.8 Hz, 2 H), 3.74 (s, 2 H), 1.07 (s, 9 H). ^{13}C{^{1}H}NMR (THF-d_8): δ 190.4, 165.3, 132.3, 131.4, 115.5, 78.8, 32.5, 26.8. IR (neat, cm^{-1}): 2957, 1690, 1604, 1576, 1510, 1477, 1365, 1313, 1256, 1216, 1160, 1046, 1014, 860, 832, 649, 616. Anal. Calcd (found) for $C_{12}H_{16}O_2$: C, 74.97 (75.05); H, 8.39 (8.49).

Kinetic Measurements. Samples for kinetic analysis were prepared from stock solutions of the appropriate palladium (aryl)halide complex and were performed in oven-dried 5 mm thin-walled NMR tubes capped with rubber septa. Solvent volume in the NMR tubes was calculated from the solvent height measured at 25 °C according to the relationship V (mL) = H (mm) × 0.01384−0.006754. Kinetic data was obtained by ^{1}H NMR spectroscopy in the heated probe of a Varian XL-300 spectrometer. Probe temperatures were measured with an ethylene glycol thermometer and were maintained at ±0.5 °C throughout data acquisition. Syringes employed in measuring liquids for kinetic measurements were calibrated by mercury displacement and were accurate to >95%. Error limits for rate constants refer to the standard deviation of the corresponding least-squares-fit line or to the standard deviation of two or more separate experiments.

(31) (a) Sakai, T.; Yasuoka, N.; Minato, H.; Kobasashi, M. *Chem. Lett.* **1976**, 1203. (b) Downie, I. M.; Heaney, H.; Kemp, G. *Angew. Chem.* **1975**, *87*, 357. (c) Danree, B.; Seyden-Penne, J. *Bull. Soc. Chim. Fr.* **1967**, 415.

(32) (a) Proudfoot, J. R.; Li, X.; Djerassi, C. *J. Org. Chem.* **1985**, *50*, 2026. (b) Reitz, A. B.; Nortey, S. O.; Maryanoff, B. E.; Liotta, D.; Monahan, R. *J. Org. Chem.* **1987**, *52*, 4191.

Thermolysis of 1b. An NMR tube containing a freshly prepared solution of **1b** (12 mg, 1.2×10^{-2} mmol) and $PhSiMe_3$ (0.70 mg, 4.6×10^{-2} mmol) in THF-d_8 (0.70 mL) was placed in the probe of an NMR spectrometer at 23 °C. The concentrations of **1b** and *p*-neopentoxybenzaldehyde were determined by integrating the *tert*-butyl resonances for **1b** (δ 0.17) and *p*-neopentoxybenzaldehyde (δ 1.06) versus the trimethylsilyl resonance of $PhSiMe_3$ (δ 0.25) in the ^1H NMR spectrum. The first-order rate constant for disappearance of **1b** was determined from a plot of $\ln\{[\mathbf{1b}]_t/[\mathbf{1b}]_0\}$ versus time (Figure 1). The presence of *p*-$HC(O)C_6H_4OCH_2CMe_3$ was confirmed by GC analysis and comparison to authentic sample. Kinetics and product analysis for thermolysis of complexes **1c**−**h** were performed analogously.

Acknowledgment. We thank the National Science Foundation, Dow Chemical, and Pfizer for their support of this work. R.W. was an NCI Postdoctoral Trainee supported by NIH Cancer Training Grant CI T32CA09112.

JA9806581